ACS OMEGA

http://pubs.acs.org/journal/acsodf

Article

Effective Modified Xanthan Gum Fluid Loss Agent for High-Temperature Water-Based Drilling Fluid and the Filtration Control Mechanism

Wenxi Zhu and Xiuhua Zheng*

Cite This: *ACS Omega* 2021, 6, 23788−23801

Read Online

ACCESS | Metrics & More | Article Recommendations

ABSTRACT: Xanthan gum (XG) was widely used as an oilfield chemical treatment agent because of its environmental protection and diverse functions. With the increased drilling depth and formation complexity, the shortcomings such as poor solubility and low resistance to temperature were gradually exposed. In this study, a modified XG derivative XG-*g*-AAA was synthesized by grafting XG with acrylic acid (AA), acrylamide (AM), and 2-acrylamido-2-methylpropane sulfonic acid (AMPS). The chemical structure of XG-*g*-AAA was determined by Fourier transform infrared spectroscopy and nuclear magnetic resonance (^{1}H NMR). Then, the solubility, high-temperature rheology and filtration properties, resistance to Na^+/Ca^{2+}, and compatibility were investigated. Results show that (1) both in aqueous and salt solutions, XG-*g*-AAA can completely be dissolved within 15 min. The significant improvement of the solubility of XG-*g*-AAA makes it more suitable for field use. (2) XG-*g*-AAA is less sensitive to high temperatures, and the viscosity decay decreased by 23.3 and 21.3% than XG at 150 and 180 °C, respectively. XG-*g*-AAA-based drilling fluid is a high-quality drilling fluid with significant shear thinning behavior, and the power-law model is the optimal model to describe its high-temperature rheology. Within 150 °C, 1.5% XG-*g*-AAA can maintain a reasonable value of the flow behavior index (n) (0.55−0.69), filtration volume (<11.6 mL), and sufficient gel strength (GS). At 150−200 °C, 3% XG-*g*-AAA is recommended. The value of n was in the range of 0.45−0.62, and the fluid loss was within 10 mL. However, 3% XG-*g*-AAA cannot provide enough GS at 200 °C; thus, a shear strength-improving agent is recommended to be added. (3) XG-*g*-AAA showed excellent contamination tolerance and compatibility. It could resist 2 wt % $CaCl_2$ and 35 wt % NaCl at room temperature and 0.75% $CaCl_2$ and 5% NaCl after 150 °C aging. (4) XG-*g*-AAA showed compatibility with sulfonated drilling fluids and could replace commercial fluid loss agents in the formula. Furthermore, the high-temperature fluid loss control mechanism was discussed by analyzing the effects of XG-*g*-AAA on the bentonite layer spacing, particle size distribution, stability of the colloidal system, and mud cakes.

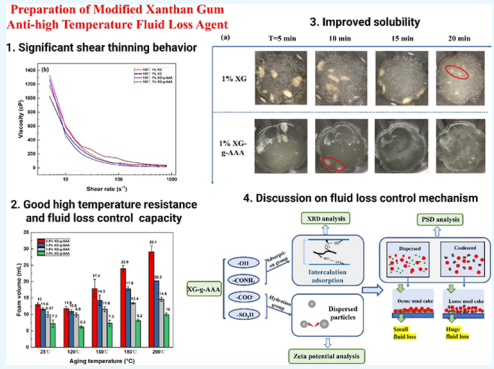

1. INTRODUCTION

Drilling fluid systems play a significant role in drilling operations, including controlling formation pressures, suspending cuttings, and cooling, as well as lubricating drilling bits. Due to the differential pressure between the formation and the wellhole, free water in drilling fluid invades the formation, causing formation damage, wellbore instability, and other complex downhole problems.[1,2] Therefore, fluid loss agents are usually added to the drilling fluid, the purpose of which is to reduce the fluid loss of the drilling fluid by forming a low-permeability, thin, and dense mud cake on the wellbore.[3,4]

As environmental protection requirements at drilling sites are becoming increasingly strict, nontoxic and degradable biopolymers such as cellulose, modified starch, and xanthan gum (XG) are receiving increasing attention and have been proven to play an active role in improving the rheological and filtration properties of drilling fluid.[5−7] XG is a natural polysaccharide biopolymer produced mainly by the bacterium *Xanthomonas campestris*.[8] Due to its good thickening and biodegradability properties, approx 30−40% of XG is currently used for oil drilling and production in the United States and Western Europe.[9] A small amount of XG can significantly increase the viscosity and adjust the flow pattern. As reported, at the same dosage (0.4%), the viscosity of the XG solution is nearly eight times that of sodium carboxymethyl cellulose (CMC).[10] Moreover, the fluid loss of XG-based mud was reduced by nearly 50% than that of CMC.[11] Although the base

Received: May 20, 2021
Accepted: August 6, 2021
Published: September 7, 2021

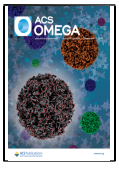

slurry containing 2% CMC maintains a good viscosity-increasing effect and a proper flow behavior index, its gel strength (GS) is 0, which is unfavorable to suspend and carry cuttings, while the GS of the base mud containing 0.5% XG reached 4.5 Pa.[12] According to the report, the effect of polyanionic cellulose on regulating fluid rheology is slightly better than CMC but still inferior to XG.[13] Moreover, the excellent thickening properties enable XG to have foam stability far beyond CMC and starch, making it a preferred choice for underbalanced drilling. Therefore, bentonite suspension based on XG is an ideal drilling fluid system.

However, the XG major issue as a treating agent of drilling fluids is its poor temperature resistance. As previously reported, the molecular structure of XG undergoes irreversible transformation above 100 °C and significant viscosity decay, which can reach more than 80% at 120 °C.[14] Zou et al. show that the shear stress of XG solution is almost 0 mPa s at different shear rates when XG solution temperature increases to 120 °C.[15] A colloidal gas aphron drilling fluid system prepared with XG shows severe fluid loss at 150 °C due to the viscosity decay of XG, and the filtration volume increased by 450% compared to 90 °C.[16] The shortage of global oil and gas reserves has prompted the exploration and development of oil and gas resources to shift to deep reservoirs. During deep well drilling, drilling fluid systems must experience long-term high temperatures (150−200 °C) and contamination of cations such as Ca^{2+} and Na^{+}, which are often accompanied by severe fluid loss invasion.[17,18] Further improvement of the temperature resistance and antipollution properties of fluid loss agents has been a constant focus of petroleum engineers.[19,20]

Numerous studies have shown that modification is an effective method to improve or obtain polymers.[21−23] Some modified polymers have been used as high-performance treatment agents.[24−27] For instance, Xiaodong Bai et al. graft acrylamide (AM) and 1-vinyl-2-pyrrolidone (NVP) onto sodium carboxymethyl starch (CMS). Results show that the product has the most excellent performance in reducing filtration volume, and the rheological performance is similar to that of CMS and better than CMC-LVT.[21] A graft copolymer KH570-AM-starch is synthesized by cassava starch (CSt), AM, and γ-methacryloxypropyl trimethoxysilane (KH570) that can be used as a fluid loss agent at 140 °C.[28] It is worth noting that KH570-AM-starch must be compounded with other agents to achieve a temperature resistance of 180 °C. As shown in Table 1, researchers have been committed to the development of new xanthan derivatives to enhance or obtain new properties and have made progress in many fields. The results showed that grafting modification changed the microscopic morphology, hydrophobic association behavior, and network structure in aqueous solution of the polymer and significantly improved the rheology and temperature resistance of XG. However, currently, the research on the temperature resistance of XG derivatives has not yet broken through the limit of high-temperature drilling (>150 °C), and it is still urgent to further enhance its high-temperature stability.

This paper aims to improve the high-temperature performance of XG by grafting rigid monomers onto XG. For this purpose, a quaternary graft copolymer XG-*g*-AA/AM/AMPS (XG-*g*-AAA) was synthesized and characterized by Fourier transform infrared spectroscopy (FT-IR), nuclear magnetic resonance (^{1}H NMR), and thermogravimetric analysis (TGA). The rheology and filtration properties of XG-*g*-AAA-based drilling fluid at selected temperatures (120−200 °C),

Table 1. Research Progress of XG and Its Derivatives

year and ref	material and method	improvement and application
2013[29]	three modified XG products XG-AMPS, XG-*g*-(AMPS-*co*-DMDAAC), and XG-*g*-(NVP-*co*-AM) were synthesized for the corresponding monomers: AM, AMPS, NVP, and dimethyl diallyl ammonium chloride (DMDAAC)	the copolymers have been successfully used as a thickener for oil well cement within 140 °C
2016[30]	XG-*g*-*N*-vinylpyrrolidone graft copolymer (XG-*g*-NVP) was prepared by ^{60}Co/γ-radiation.	XG-*g*-NVP shows higher thermal stability, and its carbonization temperature is more than 100 °C higher than that of XG. The viscosity of XG-*g*-NVP remained constant at a certain temperature (25−80 °C) and shear rate (0.1−100 s^{-1}), which effectively solved the viscosity decline of XG at elevated temperatures
2019[15]	Modified XG (MXC) was prepared via cross-linking with chromic oxalate and borax.	MXC enhanced the temperature resistance to 120 °C and has been successfully applied in the offshore exploration of Dagang oilfield, China. After aging at 120 °C, the drilling fluids of modified MXC could still maintain good theological properties and low fluid loss
2020[31]	hydrophobic long carbon chains (C16) were grafted onto the main chains of XG by etherification under the ordered conformation of xanthan	modified xanthan (XG-C16) had a better hydrophobic association effect than before. XG-C16 had better high-temperature resistance, which retained 421 mPa s at 140 °C, about four times the apparent viscosity of XG. XG-C16 also maintained a well spatial network structure in 4.0% NaCl solution and a high apparent viscosity (728 mPa s)

https://doi.org/10.1021/acsomega.1c02617
ACS Omega 2021, 6, 23788−23801

contamination tolerance ability of Ca^{2+}/Na^{+}, and compatibility in the sulfonated drilling fluid system were comprehensively investigated. To the best of our knowledge, no substantial research has been conducted on XG derivatives as fluid loss agents for water-based drilling fluids with 200 °C temperature resistance and high contamination tolerance. Additionally, the fluid loss control mechanism of XG-*g*-AAA at high temperatures was discussed through particle size distribution (PSD) analysis, X-ray diffraction (XRD) analysis, zeta potential analysis, and scanning electron microscopy (SEM).

2. METHODOLOGY

2.1. Materials. XG (AR) was a commercial reagent obtained from Tianjin Guangfu Fine Chemical Co., Ltd (Tianjin, China). XG is a light yellow powder, and the viscosity of 1% XG in water is 800−1200 mPa s. The monomers acrylic acid (AA) (>99%), AM (99%), 2-acrylamido-2-methylpropane sulfonic acid (AMPS) (98%), $NaHSO_3$ (AR), and ammonium persulfate (≥98%) were purchased from Shanghai Aladdin Biochemical Technology Co., Ltd (Shanghai, China). NaOH was purchased from Beijing Yili Fine Chemical Co., Ltd (Beijing, China). The bentonite used to prepare the base mud was obtained from Weifang Boda (Shandong, China) Bentonite Co., Ltd.

2.2. Preparation of XG-*g*-AAA. The grafting modification of XG was carried out by heating in a water bath at 55 °C under continuous nitrogen, and the product was named XG-*g*-AAA. First, the monomers AA (7.5 g)/AM (7.5 g)/AMPS (7.5 g) were dissolved in distilled water (100 mL), followed by the addition of sodium hydroxide and stirring to adjust the pH of the solution to 7−8. Then, the solution was poured into a three-necked round bottom flask. The solution was stirred with a Teflon mixing rod at a speed of ∼250 rpm. The necks at both sides were connected and discharged with nitrogen. The solution was heated (Model DF-101S) to 55 °C for 30 min under nitrogen conditions to ensure that the solution reached the temperature and the flask was filled with nitrogen. Subsequently, a certain amount of XG (2 g), ammonium persulfate (0.06 g), and sodium bisulfite (0.02 g) was added to the flask to initiate the reaction. The reaction lasted for 2 h until a light-yellow gelatinous product was obtained. The products were dried at 65 °C for 48 h and then ground into powder.

2.3. Preparation and Property Tests of Drilling Fluids. Preparation of drilling fluids: (1) the base mud was prepared by mixing bentonite (150 g), Na_2CO_3 (10 g), and 5 L of fresh water at 800 rpm for 30 min and then stirred at 450 rpm and aged for 24 h at room temperature. (2) 350 mL of base mud was taken, and a certain number of XG-*g*-AAA (0.5−3%) and XG (0.5%) were dissolved with stirring at 6000 rpm for 20 min using a high-speed mixer (Model WT-2000, China). For the contamination tolerance test mud, a certain amount of NaCl/$CaCl_2$ was added to the prepared fluid and stirred at 6000 rpm for 5 min. (3) The prepared drilling fluid was transferred to an aging pot, put into a rolling oven (Model XGRL-4, China), and aged at the selected temperatures (120, 150, 180, and 200 °C). Then, it was taken out after aging for 16 h.

Rheological tests: the rheology and filtration properties of drilling fluids were tested based on American Petroleum Institute (API) specifications and Chinese standard SY/T5621-93.[32] A six-speed rotational viscometer (Model ZNN-D6, China) was used to test the rheological properties. The prepared slurry is poured into the test cup, and readings of the viscometer at 3, 6, 100, 200, 300, and 600 rpm were recorded as φ_3, φ_6, φ_{100}, φ_{200}, φ_{300}, and φ_{600}, respectively. According to eqs 1 and 2, the measured data are transformed into shear rate (γ) and shear stress (τ). Commonly, polymer-based drilling fluid is a typical non-Newtonian fluid, and the rheology behaviors can be well described by the Bingham model, Casson model, power-Law model, and Herschel−Bulkley model. The rheological data were fitted to the four rheological models, and rheological parameters were obtained, see eqs 3−5. The high-temperature high-pressure (HTHP) rheology of drilling fluids has also been evaluated using an HTHP viscometer (Model CSL 550, China). The prepared mud (1% XG/XG-*g*-AAA-based drilling fluid) was put into an HTHP viscometer. The temperature was set to 150/180 °C, 1.5 MPa N_2 was added to prevent fluid boiling, the mud was stirred at a shear rate of 85 s^{-1}, and the fluid viscosity during the heating process (30 min) was recorded. Then, the change in fluid viscosity with the shear rate was tested by adjusting the shear rate in the range of 5−800 s^{-1}.

$$\gamma(s^{-1}) = \text{rotational speed (rpm)} \times 1.703 \quad (1)$$

$$\tau = 0.511 \times \varphi \quad (2)$$

$$\text{Bingham model: } \tau = \tau_0 + \mu_p\gamma \quad (3)$$

$$\text{Casson model: } \tau^{0.5} = \tau_0 + K\gamma^{0.5} \quad (4)$$

$$\text{Power law model: } \tau = K\gamma^n \quad (5)$$

$$\text{Herschel−Bulkley model: } \tau = \tau_0 + K\gamma^n \quad (6)$$

where τ is shear stress, γ is shear rate, φ is the reading of the six-speed viscometer, τ_0 is yield point, μ_p is plastic viscosity, n is the flow behavior index, and K is the consistency index. Parameters constrain: $\tau_0 \geq 0$; $0 < n < 1$; $K > 0$.

Filtration test: the API filtration test was carried out in a filtration apparatus (Model SD-3, China) with a stainless-steel container. The slurry was put into a container with a bottom opening, and the fluid loss was recorded within 30 min as the API filtrate volume. The top of the container is connected to the N_2 system to ensure that the mud is exposed to a pressure of 100 psi (0.69 MPa) during the test. Then, the HTHP filtration apparatus (Model HTD GS500, China) was used to record the HTHP fluid loss. The slurry was poured into the apparatus, and we set the temperature at 180 °C and the differential pressure at 3.5 MPa. We wait for the equipment temperature to increase to 180 °C and record the fluid loss volume within 30 min.

The static filtration equation describes the influencing factors of fluid loss, as shown in eq 7, where dV_f/dt is the filtration rate; K is the permeability of the mud cake; A is the cross-sectional area; Δp is the pressure differential, which is 100 psi in the API filtration test; μ is the mud viscosity; and h is the thickness of mud cake.

$$dV_f/dt = KA\Delta p/\mu h \quad (7)$$

2.4. Characterization. *2.4.1. NMR Measurements and FT-IR Spectroscopy.* ^{1}H NMR spectral analysis of the grafted copolymer XG-*g*-AAA was recorded on a JNM-ECA 600. FT-IR spectra were recorded with a Magna-IR 560 spectrophotometer at 25 °C. For each sample, 16 scans were recorded between 4000 and 400 cm^{-1} with a resolution of 4 cm^{-1}.

2.4.2. Thermogravimetric Analysis. A differential thermal thermogravimetric analyzer (Model TGA Q5000, America)

https://doi.org/10.1021/acsomega.1c02617
ACS Omega 2021, 6, 23788−23801

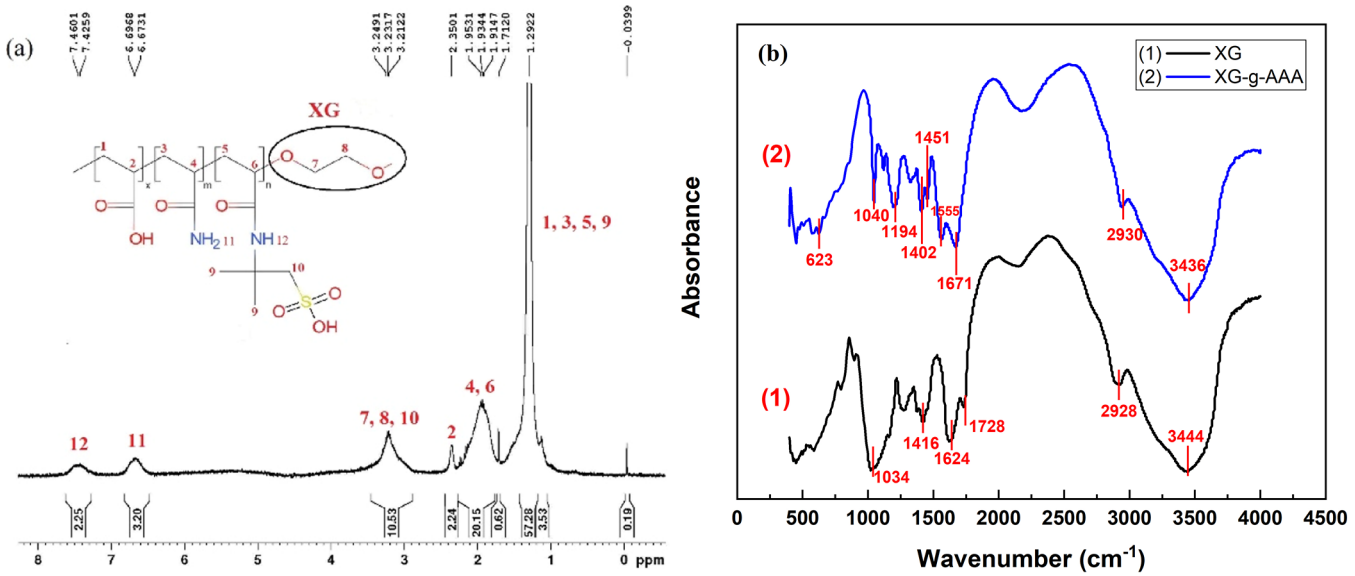

Figure 1. (a) ^{1}H NMR spectra of XG-*g*-AAA and (b) FT-IR spectra of XG-*g*-AAA.

was used to investigate the thermal stability of XG and XG-*g*-AAA under a nitrogen atmosphere at a heating rate of 10 °C/min and a temperature range of 25−600 °C.

2.4.3. Solubility Test. A certain amount of NaCl/$CaCl_2$ was added to the fresh water and stirred in a high-speed mixer at 8000 rpm for 5 min to prepare a solution containing 5% NaCl or 2% $CaCl_2$. 1% XG-*g*-AAA or 1% XG was added to freshwater, 5% NaCl, or 2% $CaCl_2$ solutions at one time and stirred at 8000 rpm. Then, we photographed the solution at certain intervals to compare the solubility of the polymers.

2.4.4. XRD Measurements. The base mud containing XG or XG-*g*-AAA, base mud containing XG or XG-*g*-AAA, and 0.5% $CaCl_2$/5% NaCl which were aged at 180 °C were dried in a 65 °C oven for 5 days and ground to powders. The powdered sample was sieved through 300 meshes and pressed into the square template; then, the measurement was carried out in an XRD instrument (Model D/max-rA Rigaku). The scanned angle (2θ) was from 3 to 10°, and the scan speed is 4°/min. The layer spacing of bentonite was calculated using Bragg's equation, see eq 8.[33]

$$d = n\lambda/2 \sin\theta \quad (8)$$

where n = 1 and λ = 1.5406 Å.

2.4.5. PSD Analysis. The aged drilling fluids were gradually poured into the tank of a laser diffraction particle size analyzer (Model Bettersize 2000, China) until the shading rate reaches 10−15%, and the equipment starts to ultrasonically disperse the sample and test the PSD.

2.4.6. Zeta Potential Analysis. The base mud containing 1% XG/XG-*g*-AAA, base mud containing 1% XG/XG-*g*-AAA, and 0.5% $CaCl_2$/5% NaCl, which were at room temperature or aged at 180 °C, were prepared. A small amount of the six samples were placed into a U-tube container, and then, we test it in a zeta potential analyzer (Model Malvern, UK).

2.4.7. Scanning Electron Microscopy. After the API filtration test, the mud cake was rinsed slowly with distilled water, dried at 65 °C for 24 h, and cut into squares 0.5 cm × 0.5 cm. The dried and cut samples were adhered to conductive tapes and metal-sprayed for 2 min. Then, SEM analysis of mud cakes was carried out using a scanning electron microscope (Model JSM-7401, Japan).

3. RESULTS AND DISCUSSION

3.1. Characterization of XG-*g*-AAA. *3.1.1. ^{1}H NMR and FT-IR.* Figure 1a shows the ^{1}H NMR spectrum of XG-*g*-AAA. The structural formula of XG-*g*-AAA and the corresponding peaks were labeled (1−10). All the peaks were assigned to the formula. It is worth noting that the peak positions of ^{1}H at multiple positions in the sample structure are close, and there is no obvious separation. Therefore, several large peaks in the spectrum contain ^{1}H at multiple positions. The peaks appearing at 6.5−7.5 ppm correspond to two amide bonds. The sulfonic acid group ($-SO_3H$) in AMPS is an electron-withdrawing group, and it will move the hydrogen on the amide to a low field, so the peaks at 7.46 and 6.69 ppm correspond to the hydrogen of the amide of AMPS and AM, respectively. XG is a kind of macromolecular substance, and the peaks in the ^{1}H NMR spectrum are not good. Generally, a bulging peak appears around 3−4.

The FT-IR spectra of the region at around 400−4000 cm^{-1} of XG and XG-*g*-AAA are shown in Figure 1b. For the curve of XG (curve a), a strong and wide absorption peak of O−H stretching vibration appeared at 3444 cm^{-1}. At 2928 cm^{-1}, there was a stretching vibration absorption peak of $-CH_2-$.[30] 1034 and 1416 cm^{-1} were the bending vibration absorption peaks of O−H and C−H, respectively. The absorption peaks that appeared at 1624 and 1728 cm^{-1} were caused by symmetric and asymmetric stretching vibration of C═O. These results are in agreement with reported data.[34−36] For the XG-*g*-AAA curve (curve b), the peaks at 1040 and 2930 cm^{-1} are characteristic absorption peaks of XG retained by the graft copolymer. The broad absorption band at 3436 cm^{-1} was due to the overlap of O−H stretching of XG and N−H stretching of AM.[23] The peak at 1402 cm^{-1} was the asymmetric vibration absorption peak of $-COO^-$ in AA;[37] 1451 cm^{-1} was the stretching vibration absorption peak of C−N in AM, while those at 1671 and 1555 were the absorption peaks of amide band I (C═O stretching vibration) and amide band II (N−H bending vibration), respectively.[22] The peaks at 623 and 1194 cm^{-1} were the absorption peaks of C−S and S═O, respectively, which characterizes the special sulfonic groups ($-SO_3H$) in AMPS.[38] Moreover, in the curve of XG-*g*-AAA,

https://doi.org/10.1021/acsomega.1c02617
ACS Omega 2021, 6, 23788−23801

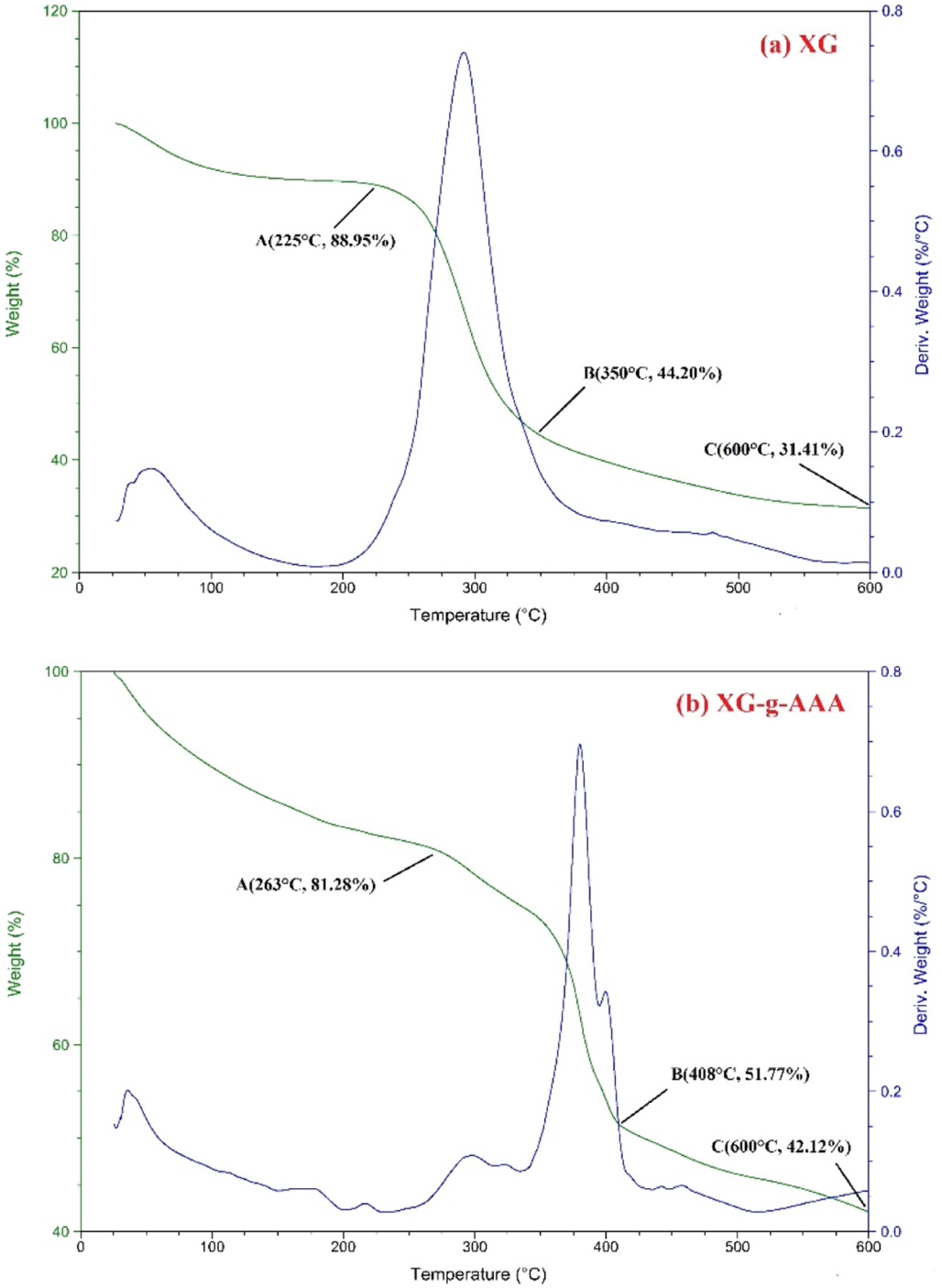

Figure 2. TGA and DTG curves of (a) XG and (b) XG-*g*-AAA.

no characteristic absorption peak of vinyl was found in the range of 910−990 cm^{-1}, indicating that no unreacted acrylic acid and AM monomer remained in the product. No characteristic absorption of C═C in AMPS was found in the range of 1600−1640 cm^{-1}.[17] Based on ^{1}H NMR and FT-IR analysis, all functional monomers have been successfully incorporated onto XG during the polymerization process.

3.1.2. Thermogravimetric Analysis. TGA and derivative thermogravimetry (DTG) curves of XG-*g*-AAA in the 25−600 °C temperature range are shown in Figure 2. Similar to XG, the thermal spectrum of XG-*g*-AAA showed three degradation steps, wherein the first stage of weight loss of about 18.7% occurred in the temperature range of 25−263 °C, which was attributed to the evaporation of free water and bound water contained in the sample. Additionally, within this temperature range, the structure of the polymer remained stable. The major weight loss of XG-*g*-AAA (29.51%) is the second step within the temperature range of 263−408 °C. This step was mainly due to the thermal decomposition of the branched groups. For instance, the graft monomers AA and AMPS contain a large number of carboxyl groups, which are released as CO_2 by thermal decomposition.[39,40] The major weight loss of XG as high as 44.75% occurred at 225−350 °C due to the polysaccharide backbone. The third degradation step of XG-

https://doi.org/10.1021/acsomega.1c02617
ACS Omega 2021, 6, 23788−23801

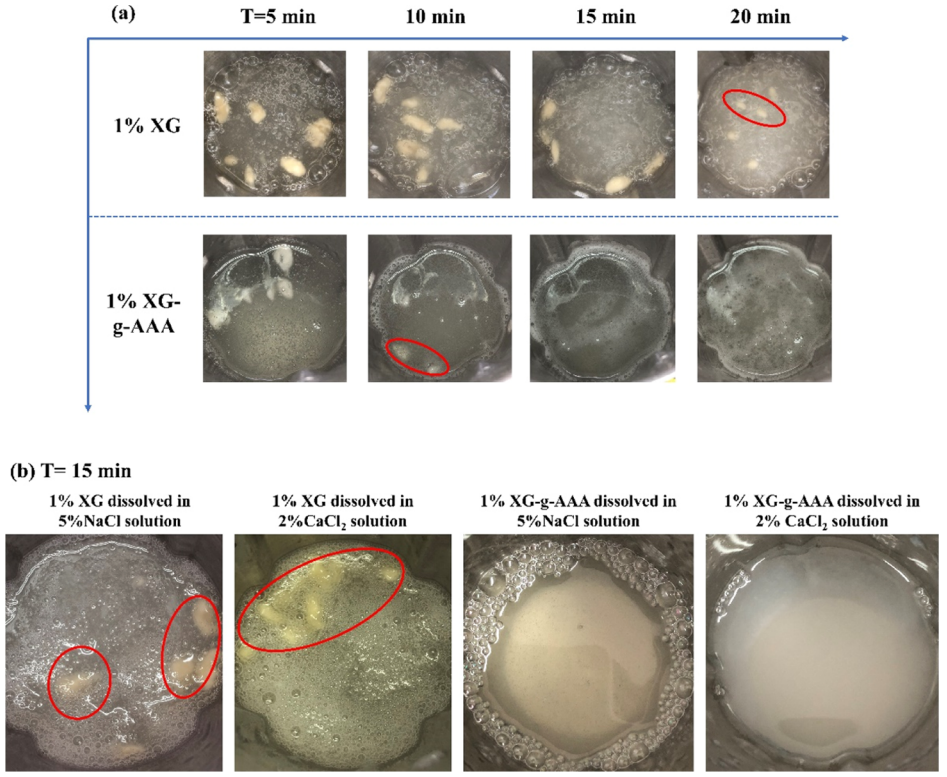

Figure 3. Solubility of XG and XG-*g*-AAA: (a) in freshwater and (b) in salt solutions.

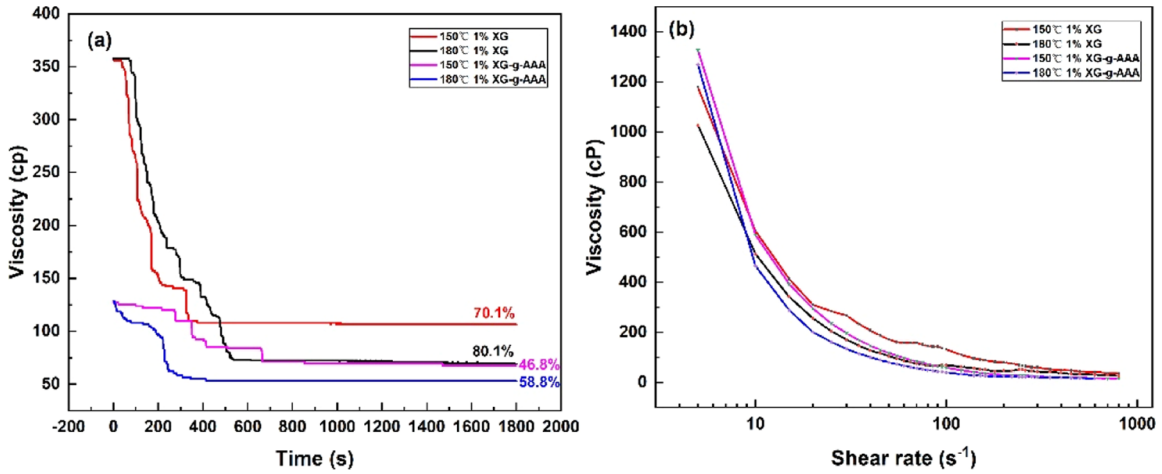

Figure 4. HTHP rheology of 1% XG and 1−3% XG-*g*-AAA: (a) viscosity vs time and (b) viscosity vs shear rate.

g-AAA occurred at 408−600 °C, where the C−C bond of the polymer backbone began to cleave, generating a weight loss of 9.65%. The maximum decomposition rate and total weight loss of XG-*g*-AAA were different from those of XG. Based on the DTG curve, XG-*g*-AAA exhibited a maximum decomposition rate at 380 °C, whereas that of XG was at 292 °C. The total weight loss of XG-*g*-AAA at 600 °C was 57.88%, which was 10.71% less than XG.

3.1.3. Solubility. The solubility is important for the use of additives in drilling fluids. The low solubility rate will prolong the time it takes to prepare the drilling fluid and reduce the drilling efficiency. Therefore, polymers that dissolve quickly in drilling fluids are the more preferred choice. Figure 3 shows a comparison of the solubility of 1% XG and 1% XG-*g*-AAA solutions. The agent was added to 300 mL of freshwater/5% NaCl solution/2% $CaCl_2$ solution at one time, continuously stirred using a high-speed mixer at 8000 rpm, and photographed.

It can be seen from Figure 3a that after XG-*g*-AAA is stirred for 5 min, clear white solids were still suspended in the water; however, after 10 min, only a small amount of white solid is observed. At t = 15 min, there were no particles in the solution. Hence, XG-*g*-AAA was completely dissolved in 10−15 min. A large number of agglomerates appeared after XG powder was added to the freshwater. Although the number and volume of agglomerates decreased as the stirring time increased, the XG solution did not dissolve well within 15 min. A small amount of yellowish solid was still suspended in water when the stirring time continually increased to 25 min. As Figure 3b shows, when the salt solution containing XG was stirred for 15 min,

https://doi.org/10.1021/acsomega.1c02617
ACS Omega 2021, 6, 23788−23801

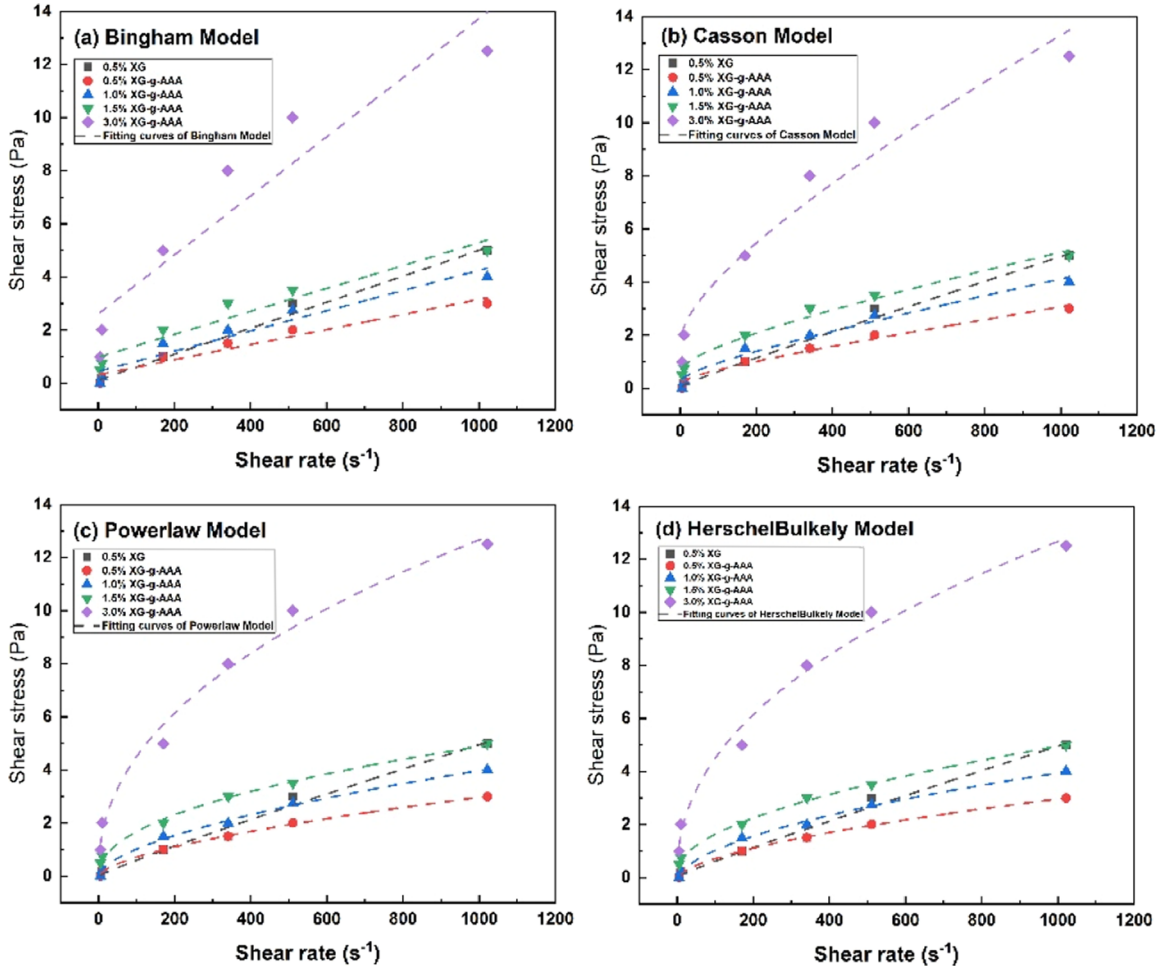

Figure 5. Fitting curves of four rheological models to 180 °C aged XG/XG-*g*-AAA-based drilling fluid: (a) Bingham plastic model; (b) Casson model; (c) power-law model; and (d) Herschel−Bulkley model.

Table 2. R^2 and RMSE of Four Rheological Models in Fitting Drilling Fluids of Different Aging Temperatures (25−200 °C)[a]

fitting parameters	model	#1	#2	#3	#4	#5
R^2	Bingham	0.884−0.987	0.947−0.980	0.935−0.989	0.925−0.981	0.892−0.960
	Casson	0.979−0.991	0.980−0.994	0.974−0.996	0.972−0.994	0.956−0.987
	power-law	0.976−0.994	0.997−0.998	0.990−0.999	0.991−0.999	0.988−0.999
	Herschel−Bulkley	0.983−0.999	0.997−0.999	0.997−0.999	0.992−0.999	0.988−0.999
RMSE	Bingham	0.21−1.56	0.23−2.08	0.28−4.22	0.18−7.14	0.34−14.70
	Casson	0.20−0.66	0.13−1.26	0.16−2.53	0.10−4.34	0.20−9.24
	power-law	0.16-0.59	0.06−0.36	0.10−0.57	0.10−1.00	0.15−2.70
	Herschel−Bulkley	0.14−0.39	0.06−0.23	0.08−0.27	0.07−0.50	0.13−1.01

[a]Formula #1: 3% bentonite base mud + 0.5% XG. Formula #2: 3% bentonite base mud + 0.5% XG-*g*-AAA. Formula #3: 3% bentonite base mud + 1.0% XG-*g*-AAA. Formula #4: 3% bentonite base mud + 1.5% XG-*g*-AAA. Formula #5: 3% bentonite base mud + 3.0% XG-*g*-AAA.

the visible yellowish solid still existed, while the solution prepared by XG-*g*-AAA was completely dissolved. Therefore, the solubility of XG in both aqueous and salt solutions is poor. The significant improvement of the solubility of XG-*g*-AAA makes it more suitable for field use.

3.2. High-Temperature Performance of XG-*g*-AAA in Drilling Fluids. *3.2.1. Rheological Property.* The HTHP rheometer records the viscosity change in the 1% XG/XG-*g*-AAA-based drilling fluid during the heating process, as well as the variation curve of fluid viscosity with the shear rate, as shown in Figure 4. As shown in Figure 4a, when the prepared fluid is heated from room temperature to the selected temperature (150/180 °C), there is a certain degree of viscosity decay in the first 15 min, and then, the viscosity value remains stable at 15−30 min. The viscosity decay of 1% XG-based drilling fluid at 150 and 180 °C reached 70.1 and 80.1%, respectively. The viscosity decay of 1% XG-*g*-AAA-based drilling fluid is 46.8 and 58.8% at 150 and 180 °C, which decreased by 23.3 and 21.3% than XG, respectively. Consequently, XG-*g*-AAA shows higher temperature resistance under the same dosage. Figure 4b shows that the fluid viscosity decreased rapidly with the increase in shear rate from 5 to 100 s^{-1} and then decreased slightly with the increase in shear rate to 800 s^{-1}. It indicates that XG/XG-*g*-AAA-based drilling fluid has shear-thinning behavior at high temperatures. Shear-thinning behavior is a necessary property of high-quality

https://doi.org/10.1021/acsomega.1c02617
ACS Omega 2021, 6, 23788−23801

drilling fluids. Drilling fluid should have low viscosity at a high shear rate for the convenience of mixing and pumping. The shear rate in the annulus is low, and the drilling fluid with high viscosity is helpful in carrying cuttings. The strength of shear-thinning behavior can be quantitatively discussed by studying the rheological model and rheological parameters.

The Bingham plastic model, Casson model, power-law model, and Herschel−Bulkley model were used to fit the relationship between shear stress and shear rate. The rheology behaviors of 0.5% XG and 0.5−3% XG-*g*-AAA-based drilling fluids at room temperature and high temperatures were investigated. The goodness of fit is expressed by R^2 and root mean square error (RMSE). A higher value of R^2 (close to 1) and a lower value of RMSE (close to 0) indicate a higher fitting accuracy. The fitting curves and parameters are shown in Figure 5 and Table 2. The results show that the relationship between shear stress and shear rate of XG/XG-*g*-AAA-based drilling fluid is not linear. Therefore, the linear equation of the Bingham plastic model exhibits the lowest fitting accuracy. The R^2 of the Bingham plastic model was as low as 0.884, and the RMSE achieved 14.7. The Casson Model comes next. For drilling fluids with different formulations and aging temperatures, the value of R^2 ranges from 0.956 to 0.996, and the RMSE ranges from 0.1 to 9.24. Both the Herschel−Bulkley model (R^2: 0.983−0.999 and RMSE: 0.06−1.01) and the power-law model (R^2: 0.976−0.999 and RMSE: 0.06−2.7) can well describe the rheological behavior of high-temperature drilling fluids. The Herschel−Bulkley model introduced the yield point to better fit the rheological curve at low shear rates and has higher fitting accuracy. However, the Herschel−Bulkley model shows a negative τ_0 when fitting multiple sets of high-temperature drilling fluids, as shown in Table 3. This

Table 3. Negative Rheological Parameters of the Herschel−Bulkley Model in Fitting Drilling Fluid at Different Aging Temperatures

T/°C	formula	τ_0	n	K
120	#4	−0.17	0.62	0.54
	#5	−2.90	0.57	2.51
150	#1	−0.15	0.82	0.02
	#5	−1.85	0.60	1.68
180	#2	−0.04	0.60	0.05
	#3	−0.17	0.54	0.10

violates the premise of the Herschel−Bulkley model. In previous reports, the same problems appeared when fitting high-temperature microbubble drilling fluids and drilling fluids containing nanoparticles. Therefore, considering the fitting accuracy and reasonable rheological parameters, the power-law model is the optimal model to describe the rheological behavior of high-temperature XG-*g*-AAA-based drilling fluids.[16,41]

The rheological parameters of the power-law Model are listed in Table 4. The smaller the value of the flow behavior index (n), the stronger the non-Newtonian properties of the drilling fluid. To ensure that the drilling fluid has good shear thinning properties, it is necessary to reduce the value of n. Generally, the value of n within 0.7 is reasonable. Increasing the consistency index (K) value is conducive to carrying cuttings.[42] Compared with 0.5% XG, 0.5% XG-*g*-AAA always has a higher K value and a lower n value. XG-*g*-AAA also has a higher GS ($GS_{10\ min}$) at high temperatures, corresponding to a

Table 4. Rheological Parameters for XG and XG-*g*-AAA at Different Aging Temperatures Using the Power-Law Model

T/°C	formula	n	K	R^2	RMSE	$GS_{10\ min}$ (Pa)
25	#1	0.19	5.15	0.9834	0.59	7.5
	#2	0.62	0.35	0.9984	0.36	1
	#3	0.58	0.88	0.9988	0.57	1.5
	#4	0.55	1.73	0.9985	1.00	3.5
	#5	0.54	3.47	0.9972	2.70	5.1
120	#1	0.79	0.04	0.9756	0.47	1.0
	#2	0.69	0.11	0.9965	0.27	2.1
	#3	0.64	0.29	0.9960	0.52	2.1
	#4	0.63	0.51	0.9987	0.50	3.1
	#5	0.60	2.00	0.9993	1.19	4.5
150	#1	0.86	0.02	0.9943	0.16	0
	#2	0.74	0.05	0.9969	0.15	0.5
	#3	0.72	0.06	0.9904	0.26	1.0
	#4	0.69	0.09	0.9912	0.34	1.5
	#5	0.62	1.39	0.9994	0.88	3
180	#1	0.92	0.01	0.9856	0.21	0
	#2	0.62	0.04	0.9967	0.06	0.5
	#3	0.59	0.07	0.9949	0.10	0.5
	#4	0.46	0.20	0.9954	0.11	1.0
	#5	0.45	0.57	0.9882	0.45	2
200	#4	0.695	0.03	0.9939	0.10	0.3
	#5	0.61	0.07	0.9926	0.15	0.5

stronger ability to suspend cuttings, while the $GS_{10\ min}$ of XG decreased to 0 when the temperature exceeds 150 °C. As indicated by Darley and Gray,[43,44] any clay-based drilling fluid should have a GS of 3 lb/100 ft^2 (1.44 Pa). Therefore, compared with XG, XG-*g*-AAA can significantly improve the high-temperature rheological properties.

The polymer molecules attach to the clay surface through the adsorption group to play a role. The adsorption group of XG tends to desorb and separate from the clay particles at high temperatures. XG-*g*-AAA introduces a high-temperature resistant group ($-SO_3H$) to enhance the temperature resistance of the molecular chain. As the concentration of XG-*g*-AAA increased, more functional groups attach to the clay particles and play a role, resulting in a decrease in n value and an increase in K value and $GS_{10\ min}$. For this reason, increasing the concentration of XG-*g*-AAA enhanced the shear thinning behavior and improved the ability to carry and suspend cuttings. Within 150 °C, 1.5% XG-*g*-AAA can maintain a reasonable value of n and sufficient $GS_{10\ min}$. At 150−180 °C, 3% XG-*g*-AAA is recommended. At 200 °C, 3% XG-*g*-AAA cannot provide enough GS; thus, a shear strength-improving agent is recommended to be added in the drilling fluid system.

3.2.2. Filtration Property. Filtration and well-building properties are one of the most important properties of drilling fluids. The larger the filtration volume is, the worse is the wellbore stability and formation protection. According to the API standard, the filtration volume of drilling fluid before and after aging should be less than 15 mL within 30 min.[17,32,45]

The filtration property of base mud containing XG-*g*-AAA was studied after aging at selected temperatures (120−200 °C) to evaluate its application in a water-based drilling fluid system as a fluid loss agent. Each formulation had been tested in triplicate, and the results are shown in Figure 6. Mud with 0.5% XG was the control group, which was not marked in Figure 6 due to its large value. The FL_{API} of 0.5% XG was 95 mL at 150 °C. The complete filtration occurred at 200 °C, and

https://doi.org/10.1021/acsomega.1c02617
ACS Omega 2021, 6, 23788−23801

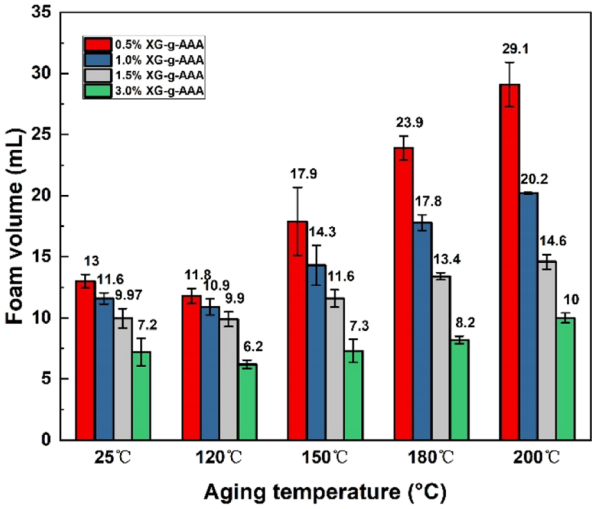

Figure 6. API filtration volume of base mud with different concentrations of XG-*g*-AAA at appointed temperatures.

the FL_{API} was more than 200 mL. XG failed to control the fluid loss at the temperature exceeding 150 °C, and it is not recommended for use in high-temperature drilling.

The fluid loss of base mud with 0.5% XG-*g*-AAA at 120, 150, and 180 °C was 11.8, 17.9, and 23.9 mL, respectively, which decreased by 63.7, 81.2, and 87.1%, compared to XG. After modification, the improvement on the high-temperature fluid loss control ability of XG is obvious. When the aging temperature was below 150 °C, fluid loss of 1.0% XG-*g*-AAA could be controlled within 15 mL. Increasing XG-*g*-AAA concentration is conducive to reduce the filtration volume. As XG-*g*-AAA concentration increased to 1.5%, the filtration volume could be controlled within an acceptable range (≤14.6 mL) at 200 °C. When the dosage of XG-*g*-AAA is increased to 3%, the FL_{API} at 200 °C can be further reduced to 10 mL.

Further testing was carried out for the HTHP filtration volume of based mud with 3% XG-*g*-AAA at 150/180 °C, and the results are shown in Table 5. The FL_{HTHP} of bentonite-based mud at 150/180 °C is a complete loss. At 150 and 180 °C, XG-*g*-AAA could significantly reduce the HTHP filtration volume of the base slurry and the FL_{HTHP} of 3% XG-*g*-AAA at 150/180 °C was 16.8 and 24.5 mL, respectively. Table 5 also lists the FL_{API} and FL_{HTHP} of two high-temperature-resistant polymer fluid loss agents in the previous literature as a comparison. Both the FL_{API} and HTHP results demonstrated that XG-*g*-AAA played a significant role in controlling filtration volume, even if after aging at high temperatures.

Table 5. Filtration Volume of 3% XG-*g*-AAA and Comparison to Reported Fluid Loss Agents

	150 °C		180 °C	
formula	FL_{API} (mL)	FL_{HTHP} (mL)	FL_{API} (mL)	FL_{HTHP} (mL)
3% XG-*g*-AAA	7.3	16.8	8.2	24.5
1.5% PAMAP[46]	~10	~30	>15	>40
2% AM/AMPS polymer[45]	11.2	17.6	22	31.8

According to eq 7, under the condition of a constant pressure difference (Δp = 0.69 MPa) and filtration area (A), thickness (h) and permeability (K) of mud cake were the main factors affecting filtration loss. The thinner and denser the mud cake, the lower the filtration volume. Figure 7a,b shows the mud cake of drilling fluid with XG and XG-*g*-AAA after aging at 150 °C. The mud cake of XG slurry (Figure 7a) was very loose and up to 18 mm in thickness, whereas that of XG-*g*-AAA slurry (Figure 7b) was dense and only 0.6 mm in thickness. The mud cakes were further observed by SEM. As shown in Figure 7c,d, the mud cake surface of XG−AAA was smooth, while that of XG showed obvious pores and cracks. The results confirmed that through the addition of XG-*g*-AAA, a high-quality mud cake was formed at high temperatures, effectively reducing filtration loss.

3.2.3. Ca^{2+}/Na^{+} Contamination Tolerance. The drilling fluid may be contaminated by Ca^{2+}/Na^{+} in formation during circulation in the wellbore. Therefore, Ca^{2+}/Na^{+} contamination tolerance of XG-*g*-AAA and XG was evaluated (Figure 8). At room temperature, the cation tolerance of XG-*g*-AAA reached 2 wt % $CaCl_2$ and 35 wt % NaCl. At 0.25−2 wt % $CaCl_2$, fluid loss of the mud containing 1% XG-*g*-AAA was within 10.3 mL. When NaCl concentration increased from 5 to 35 wt %, fluid loss of XG-*g*-AAA was within the range of 7.2−9.5 mL. XG showed good synergism with $CaCl_2$ and NaCl at room temperature, which is consistent with the literature. As reported,[14] high concentrations of salt ions affect the conformational transition temperature and the double helix structure of XG, which further affects the rheological and filtration properties. After adding 2 wt % $CaCl_2$ and 35 wt % NaCl, fluid loss of XG-based drilling fluid decreased from 13.2 to 7.8 and 6.2 mL, respectively.

However, at 150 °C, the filtration volume of XG-based drilling fluid increased sharply from 95 to 152 and 113 mL after the addition of 5 wt % NaCl and 0.25 wt % $CaCl_2$, respectively, indicating poor fluid loss control performance. High-temperature aging decreased the contamination tolerance of XG-*g*-AAA to a certain extent. After 150 °C aging, the filtration volume of mud with 1% XG-*g*-AAA and 0.25 wt %, 0.5 wt %, and 0.75 wt % $CaCl_2$ was 10.3, 9.4, and 19.2 mL, respectively. When the amount of $CaCl_2$ was above 0.75 wt %, the filtration loss was considerably higher than 20 mL. The fluid loss of mud containing 1% XG-*g*-AAA and 5 wt % NaCl at 150 °C was 20.8 mL. When NaCl concentration increased to 10 and 25 wt %, FL increased to 45.6 and 57.7 mL, respectively. XG-*g*-AAA could resist 0.75 wt % $CaCl_2$ and 5 wt % NaCl after aging at 150 °C.

3.2.4. Compatibility of XG-g-AAA in the Sulfonated Drilling Fluid System. A good drilling fluid treating agent needs to have good performance while being compatible and synergistic with other treating agents. Formula #1 is a drilling fluid system containing sulfonated polymers, in which the sulfomethyl phenolic resin (SMP-2) and sulfonated lignite resin (SPNH) are fluid loss agents and FA-367 is a coating agent.[47] The compatibility of XG-*g*-AAA was evaluated via direct addition to #1 or replacing the fluid loss agents in the formula. The rheological and filtration properties were evaluated (Table 6).

Formula #4 was obtained via the addition of 1% XG-*g*-AAA to #1. As shown in Table 6, compared to #1 at 180 °C, AV of #4 increased from 12 to 25.5 mPa s, and FL decreased from 14 to 7.4 mL. Compared with #1 at 200 °C, AV of #4 increased to 24 mPa s and FL reduced to 7.4 mL. Table 6 also shows that the thermal stability of #1 became worse after the addition of Ca^{2+}. When the temperature increased from 25 to 150 °C, the AV of #1 with 0.5% $CaCl_2$ decreased from 9 to 1.5 mPa s, and

https://doi.org/10.1021/acsomega.1c02617
ACS Omega 2021, 6, 23788−23801

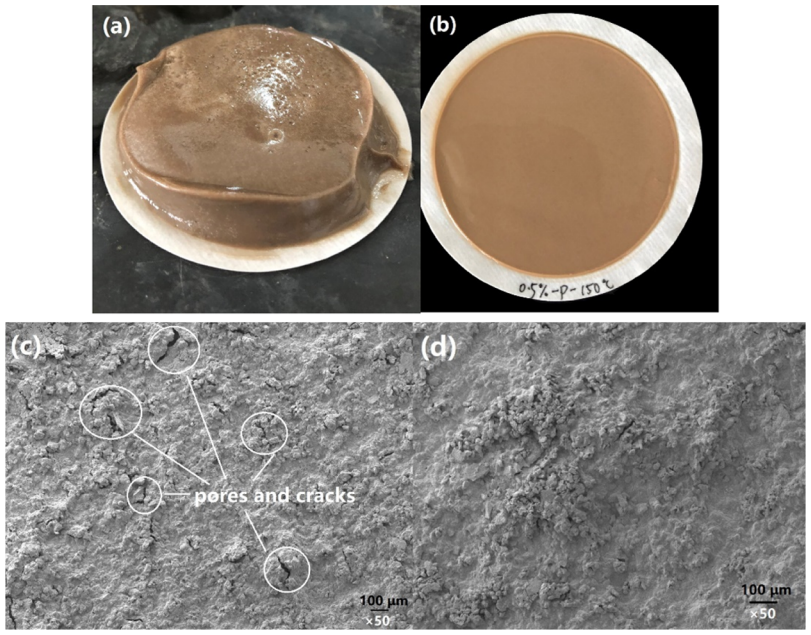

Figure 7. Mud cake images after aging at 150 °C: (a) mud cake of XG; (b) mud cake of XG-*g*-AAA; (c) SEM images of mud cakes of XG; and (d) SEM images of mud cakes of XG-*g*-AAA.

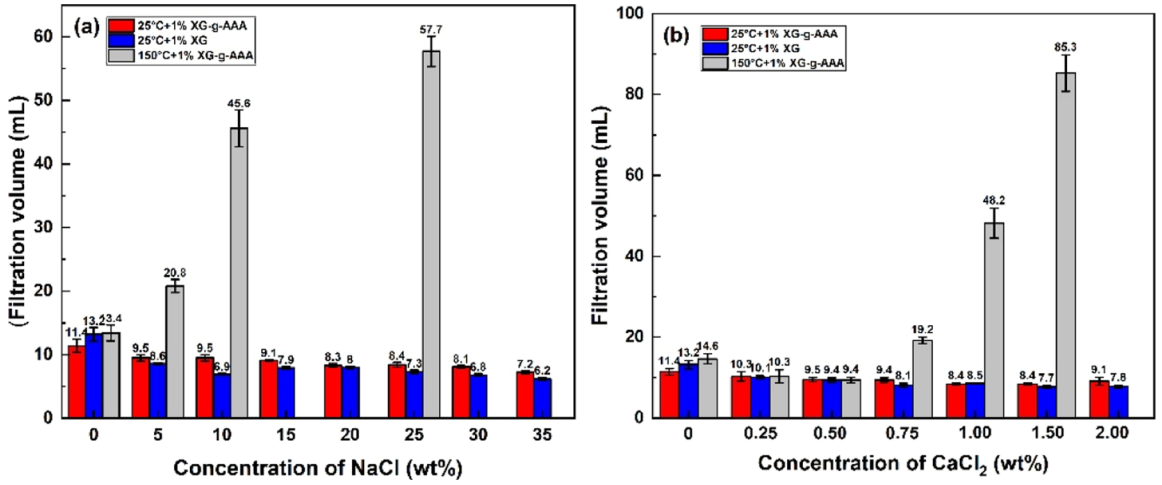

Figure 8. Fluid loss of mud with different concentrations of NaCl/$CaCl_2$. (a) 0−36 wt % NaCl. (b) 0−2 wt % $CaCl_2$.

FL increased from 16 to 52.5 mL. After adding 1% XG-*g*-AAA to #1, the cation contamination tolerance of the drilling fluid system was greatly improved. At 150 °C, AV of #4 was 9 mPa s, and FL could be controlled within 10 mL. After the addition of 5% NaCl, the performance of #4 was also improved compared to #1, at room temperature or 150 °C aging. Formulas #2 and #3 were obtained by replacing SPNH and SMP-2 in formula #1 with XG-*g*-AAA, respectively. Table 6 shows that the FL of #2 and #3 was reduced compared with #1 after high-temperature (180/200 °C) aging, which was within 10 mL.

Briefly, whether it is high-temperature aging or the addition of $CaCl_2$/NaCl, the drilling fluid system containing XG-*g*-AAA had higher apparent viscosity and lower filtration loss, which showed that XG-*g*-AAA had a good synergistic effect with the sulfonated drilling fluid system. XG-*g*-AAA can also replace the fluid loss agents in the formula.

3.3. High-Temperature Fluid Loss Control Mechanism of XG-*g*-AAA. *3.3.1. PSD Analysis.* In the filtration process, larger-sized clay particles are required as bridging particles, which are stuck in the throat of the rock pore. Clay particles with a smaller particle size are also required as filler particles to fill small pores between large particles. Therefore, reasonable PSD is conducive to improving the filtration performance of drilling fluids.[48] After aging at 180 °C, the particle size analysis of base mud and base mud with XG or XG−AAA is shown in Figure 9.

As shown in Figure 9, base mud containing XG-*g*-AAA had a wide range of PSD, which contained small particles with a diameter of 0.1−10 μm and a large particle size of 100−1000 μm. Compared with base mud and mud with XG, the main peak of XG-*g*-AAA slurry was reduced from ∼45 μm (peak 1) to ∼10 μm (peak 2). It is worth noting that the peak of XG-*g*-AAA-based mud at ∼45 μm did not disappear, which ensured that larger particles, that is, bridging particles, were present in the drilling fluid system. After addition of XG-*g*-AAA to base mud, the medium diameter was reduced from 16.04 to 9.889 μm, and the average diameter decreased from 29.44 to 19.54

https://doi.org/10.1021/acsomega.1c02617
ACS Omega 2021, 6, 23788−23801

Table 6. Apparent Viscosity and Fluid Loss of Different Formulas at Different Temperatures[a]

	AV/mPa s		FL/mL	
formula	180 °C	200 °C	180 °C	200 °C
#1	12	17.5	14	11.4
#2	24	21.5	8	9
#3	15	18	8.6	9.4
#4	25.5	24	7.4	7.4

	AV/mPa s		FL/mL	
formula	25 °C	150 °C	25 °C	150 °C
#1 + 0.5% $CaCl_2$	9	1.5	16	52.5
#4 + 0.5% $CaCl_2$	31	9	7.8	6.4
#1 + 5% NaCl	9.6	8	14.5	15.2
#4 + 5% NaCl	37.5	17	8	7

[a]Formula #1: 3% bentonite base mud + 0.1% FA-367 + 1% SMP-2 + 1% SPNH. Formula #2: 3% bentonite base mud + 0.1% FA-367 + 1% SMP-2 + 1% XG-*g*-AAA. Formula #3: 3% bentonite base mud + 0.1% FA-367 + 1% SPNH + 1% XG-*g*-AAA. Formula #4: formula #1 + 1% XG-*g*-AAA.

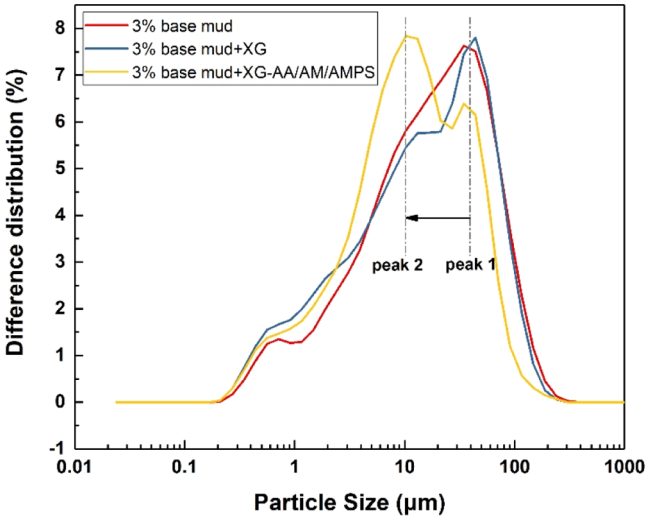

Figure 9. After aging at 180 °C, the PSD of base mud, base mud with XG, and base mud with XG-*g*-AAA.

μm. After aging at 180 °C, the addition of XG-*g*-AAA could effectively prevent the clay from coalescing into large particles and increase the content of fine particles in the drilling fluid system. These fine particles served as filling particles to fill the pores between large particles, which made the mud cake denser and had lower permeability.

3.3.2. XRD Analysis. XRD analysis is the most effective method for analyzing the clay layer spacing. The clay layer spacing varies with the hydration of the clay and intercalation of chemical substances. The larger layer spacing of the clay means better hydration and dispersion capabilities. XRD patterns and interlayer spacing (d_{001}) of bentonite with various formulas were obtained and are depicted in Figure 10. After aging at 180 °C, the layer spacing of bentonite containing XG was 12.70 Å. The clay layer spacing of mud with XG-*g*-AAA increased to 14.92 Å due to its intercalation. The addition of Ca^{2+} and Na^+ reduced the bentonite layer space. However, the layer spacing of XG-*g*-AAA mud was always greater than that of XG. After the addition of 0.5% $CaCl_2$, XG-*g*-AAA-containing bentonite layer space decreased to 12.96 Å, while that of XG was 12.38 Å. After the addition of 5% NaCl, the layer space of XG-*g*-AAA mud was 13.64 Å. The bentonite interlayer of XG-containing mud was destroyed, and the characteristic peak disappeared. In short, after the addition of $CaCl_2$/NaCl, the addition of XG-*g*-AAA significantly improved the bentonite layer space and mud containing XG-*g*-AAA was more dispersive.

3.3.3. Zeta Potential Analysis. Bentonite-based drilling fluid is a typical colloidal dispersion system with a diffusion electric double layer. Zeta potential is an important characteristic parameter of the diffusion electric double layer, which refers to the potential from the interface of the solvation layer to the homogeneous liquid phase. The thicker the electric double layer, the greater the zeta potential, the stronger the particle dispersion, and the more stable the colloid. Generally, the drilling fluid system should be stable when zeta potential absolute values are greater than 30 mV.[49]

Figure 11 shows the zeta potential of drilling fluids containing XG-*g*-AAA and XG. High temperature and the existence of Na^+/Ca^{2+} significantly reduced the zeta potential of XG, which means that the bentonite particles tend to coalesce. High temperature promotes the desorption of the treatment agent on the surface of clay particles and increases the collision frequency of the colloid. On the other hand, the introduction of counterions in the electrolyte gradually compresses the electric double layer and the zeta potential decreases. When the diffusion electric double layer is reduced to the thickness of the solvation layer, the colloid transforms

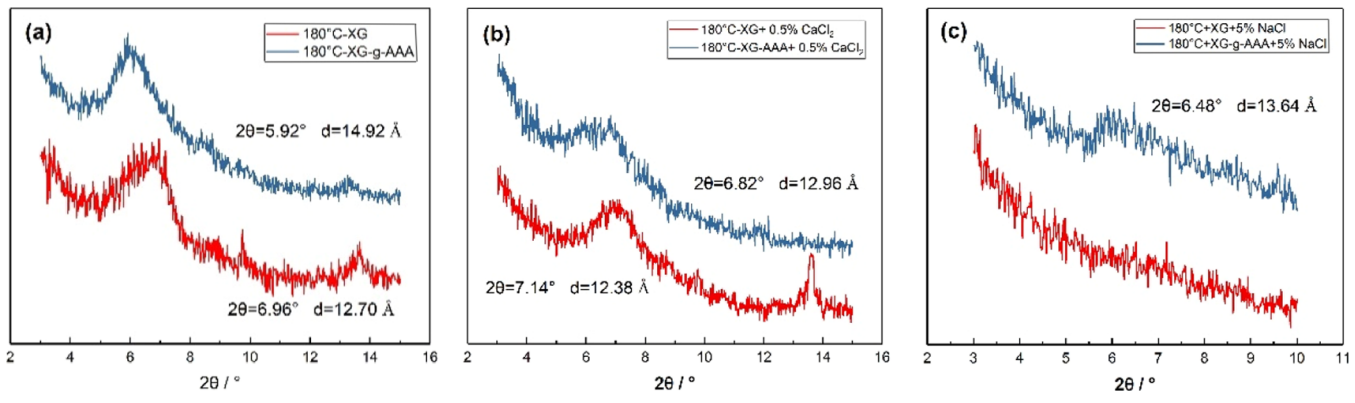

Figure 10. XRD of bentonite mud with different formulas after aging at 180 °C. (a) Mud with XG/XG-*g*-AAA. (b) Mud with 0.5% $CaCl_2$ and XG/XG-*g*-AAA. (c) Mud with 5% NaCl and XG/XG-*g*-AAA.

https://doi.org/10.1021/acsomega.1c02617
ACS Omega 2021, 6, 23788−23801

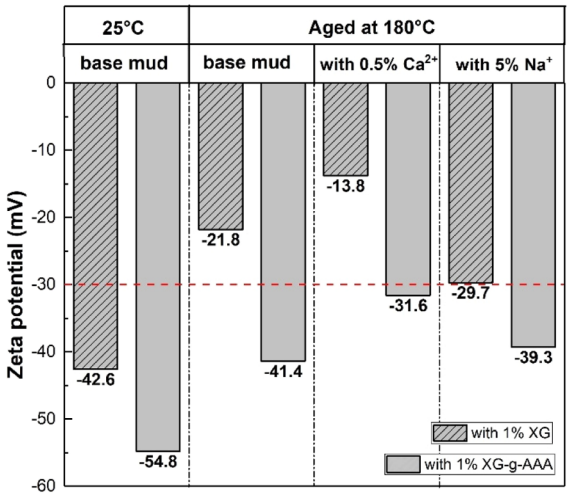

Figure 11. Zeta potential of different formulas at different temperatures.

into an isoelectric state which is easy to coalesce.[50] Before and after aging at 180 °C, the absolute value of zeta potential of XG-*g*-AAA-based drilling fluid was always greater than that of XG and was also higher than 30 mV. After aging at 180 °C and the addition of 0.5 wt % $CaCl_2$ and 5 wt % NaCl, the zeta potential absolute values of base mud containing 1% XG-*g*-AAA were between 31.6 and 41.4 mV. In other words, the XG-*g*-AAA-based slurry can maintain the dispersion and stability of colloidal particles in high temperature and electrolyte solution.

3.3.4. Fluid Loss Control Mechanism of XG-g-AAA. The FT-IR analysis proved that the grafting monomers AA, AM, and AMPS successfully introduced a large number of carboxyl groups ($-COO^-$), amide groups ($-CONH_2$), and sulfonic acid groups ($-SO_3H$) into the substrate XG. The amide group as an adsorption group can form intercalation adsorption with the Al−OH and Si−OH groups on the surface of the bentonite through hydrogen bonding. The layer spacing and dispersibility of bentonite are improved. Carboxylic and sulfonic acid groups are strong hydration groups, which help to form a strong solvation layer while improving the solubility of the polymer.[51] The existence of charged colloidal particles and solvated layer is the reason why the sol can maintain dispersion and stability for a long time. Moreover, the amide group has strong salt resistance, and the sulfonic acid group is not sensitive to high temperatures. Therefore, the introduction of functional groups effectively prevents the agglomeration and sedimentation of clay particles and improves the PSD gradation (Figure 12). Under the differential pressure, the fluid loss is controlled by forming a thin and dense mud cake .

4. CONCLUSIONS

In the present investigation, a novel quaternary copolymer XG derivative XG-*g*-AAA was synthesized, characterized, and used successfully in drilling muds at high temperatures (120−200 °C). Results show that XG-*g*-AAA can be completely dissolved in aqueous and salt solution within 15 min. The solubility of XG-*g*-AAA was significantly better than that of XG, which makes it a preferred choice for drilling sites. After high-temperature aging, XG-*g*-AAA-based drilling fluid can still show satisfactory rheology and filtration properties, while XG is not recommended for use at temperatures exceeding 120 °C. HTHP rheology shows that XG-*g*-AAA-based drilling fluids is a high-quality drilling fluid with significant shear thinning behavior and is less sensitive to high temperatures than XG. The power-law model is selected to describe the high-temperature rheology of XG-*g*-AAA-based drilling fluids considering its adequate accuracy and reasonable indexes.

Based on experimental findings, the following suggestions are proposed for the dosage of XG: Within 150 °C, 1.5% XG-*g*-AAA can maintain a reasonable value of rheological parameters, filtration volume (<11.6 mL), and sufficient GS. At 150−200 °C, 3% XG-*g*-AAA is recommended. The prepared drilling fluid has strong shear thinning properties, and the fluid loss was within 10 mL. However, 3% XG-*g*-AAA

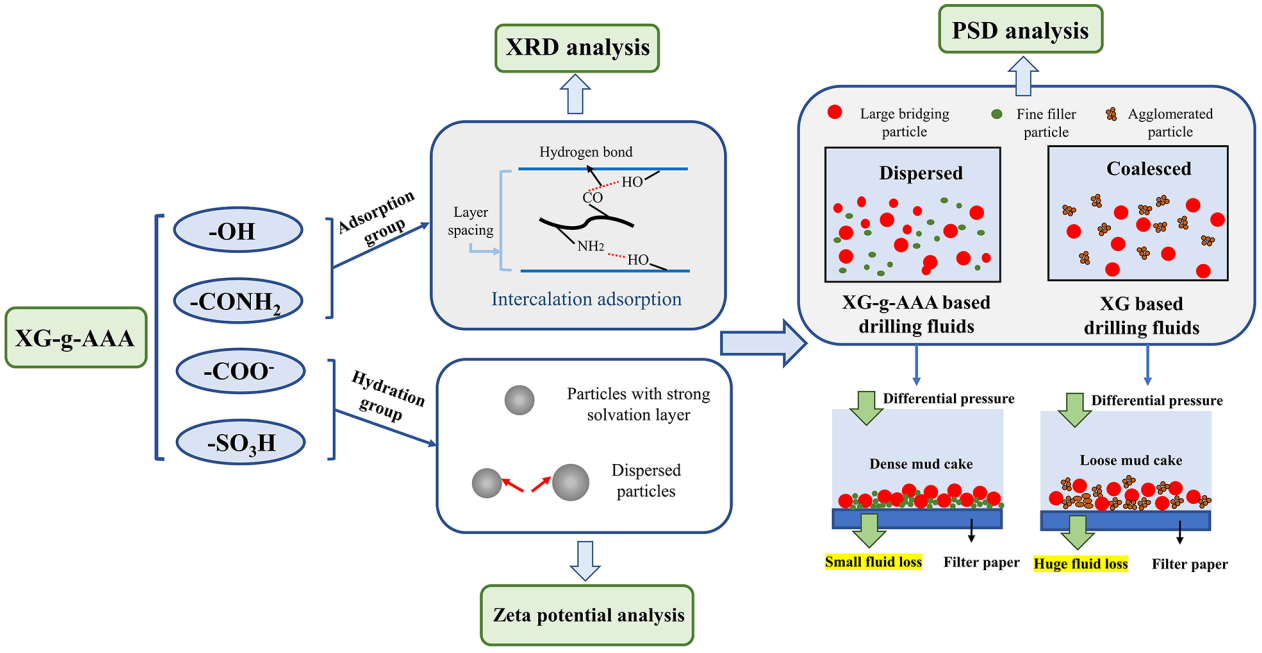

Figure 12. Fluid loss control mechanism diagram of XG-*g*-AAA.

https://doi.org/10.1021/acsomega.1c02617
ACS Omega 2021, 6, 23788−23801

cannot provide enough GS at 200 °C; thus, a shear strength-improving agent is recommended to be added.

Also, great improvement on the Ca^{2+}/Na^{+} contamination tolerance of XG-*g*-AAA was observed at room temperature and high temperature. XG-*g*-AAA shows good compatibility with the sulfonated drilling fluid system whether at high temperature or cation contamination. It could also replace the fluid loss agents SPNH or SMP-2 in the formula. Therefore, XG-*g*-AAA was found to be a promising high-temperature resistant additive for controlling rheological and fluid-loss properties in water-based drilling fluids.

The promoting properties exhibited by XG-*g*-AAA were ascribed to the introduction of a large number of functional groups, which effectively prevented the aggregation and settlement of clay particles by enhancing the adsorption and hydration, and maintained the dispersion and stability of base slurry for a long time. However, viscosity decay still exists. In the next study, the rigid ring structure and reverse emulsion polymerization will be considered to further promote the high-temperature performance of XG.

AUTHOR INFORMATION

Corresponding Author

Xiuhua Zheng − *School of Engineering and Technology, China University of Geosciences (Beijing), Beijing 100083, P.R. China;* orcid.org/0000-0002-3034-0407; Phone: +86-15911062856; Email: xiuhuazh@cugb.edu.cn

Author

Wenxi Zhu − *School of Engineering and Technology, China University of Geosciences (Beijing), Beijing 100083, P.R. China*

Complete contact information is available at: https://pubs.acs.org/10.1021/acsomega.1c02617

Author Contributions

W.Z.: methodology, data curation, and writing—original draft. X.Z.: funding acquisition and writing—review and editing.

Notes

The authors declare no competing financial interest.

ACKNOWLEDGMENTS

This work was supported by the National Natural Science Foundation of China (grant no. 41872184) of "Properties of Colloid Gas Aphron Drilling Fluid and Its Mechanism of Loss and Formation Protection for High Temperature Geothermal Reservoir".

REFERENCES

(1) Davoodi, S.; Ramazani S.A, A.; Soleimanian, A.; Fellah Jahromi, A. Application of a novel acrylamide copolymer containing highly hydrophobic comonomer as filtration control and rheology modifier additive in water-based drilling mud. *J. Pet. Sci. Eng.* **2019**, *180*, 747−755.

(2) Hamad, B. A.; He, M.; Xu, M.; Liu, W.; Mpelwa, M.; Tang, S.; Jin, L.; Song, J. A Novel Amphoteric Polymer as a Rheology Enhancer and Fluid-Loss Control Agent for Water-Based Drilling Muds at Elevated Temperatures. *ACS Omega* **2020**, *5*, 8483−8495.

(3) He, X.; Chen, Q.; Feng, C.; Wang, L.; Hou, H. Synthesis and performance of a self crosslinkable acrylate copolymer with high compatibility for an oil well cement modifier. *J. Polym. Eng.* **2014**, *34*, 405−413.

(4) Li, Z.; Pu, X.; Tao, H.; Liu, L.; Su, J. Synthesis and properties of acrylamide 2-acrylamido-2-methypropane sulfonic acid sodium styrene sulfonate N-vinyl pyrrolidone quadripolymer and its reduction of drilling fluid filtration at high temperature and high salinity. *J. Polym. Eng.* **2014**, *34*, 125−131.

(5) Baba Hamed, S.; Belhadri, M. Rheological properties of biopolymers drilling fluids. *J. Pet. Sci. Eng.* **2009**, *67*, 84−90.

(6) Liu, J.; Guo, B.; Li, G.; Wang, B.; Chai, J. Synthesis And Performance of Environmental Friendly Starch Based Filtrate Reducers For Water Based Drilling Fluids. *Fresenius Environ. Bull.* **2019**, *28*, 5618−5623.

(7) Liu, X.; Yuan, Z.; Wang, A.; Wang, C.; Qu, J.; Chen, B.; Wei, B.; Kapu, N. S.; Wen, Y. Cellulose nanofibril-polymer hybrids for protecting drilling fluid at high salinity and high temperature. *Carbohydr. Polym.* **2020**, *229*, 115465.

(8) Petri, D. F. S. Xanthan gum: A versatile biopolymer for biomedical and technological applications. *J. Appl. Polym. Sci.* **2015**, *132*, 42035.

(9) Sun, L.; Wei, P.; Fu, Q.; Zhang, J.; Zeng, D. Research advance of xanthan system with temperature resistance and salt resistant in the oilfield development. *App. Chem. Ind.* **2014**, *43*, 2279−2284.

(10) Da Luz, R. C. S.; Fagundes, F. P.; Balaban, R. D. C. Water-based drilling fluids: the contribution of xanthan gum and carboxymethylcellulose on filtration control. *Chem. Pap.* **2017**, *71*, 2365−2373.

(11) Tabzar, A.; Arabloo, M.; Ghazanfari, M. H. Rheology, stability and filtration characteristics of Colloidal Gas Aphron fluids: Role of surfactant and polymer type. *J. Nat. Gas Sci. Eng.* **2015**, *26*, 895−906.

(12) Benyounes, K.; Mellak, A.; Benchabane, A. The Effect of Carboxymethylcellulose and Xanthan on the Rheology of Bentonite Suspensions. *Energy Sources, Part A* **2010**, *32*, 1634−1643.

(13) Nwosu, O. U.; Ewulonu, C. M. Rheological Behaviour of Eco-friendly Drilling Fluids from Biopolymers. *J. Polym. Biopolym. Phys. Chem.* **2014**, *2*, 50−54.

(14) Wu, L.; Xu, T.; Han, X.; Pan, X. Research on high temperature stability effects of xanthan gum. *Drill. Fluid Completion Fluid* **2011**, *28*, 77−80.

(15) Zou, Z.; Zhao, Q.; Wang, Q.; Zhou, F. Thermal stability of xanthan gum biopolymer and its application in salt-tolerant bentonite water-based mud. *J. Polym. Eng.* **2019**, *39*, 501−507.

(16) Zhu, W.; Zheng, X.; Li, G. Micro-bubbles size, rheological and filtration characteristics of Colloidal Gas Aphron (CGA) drilling fluids for high temperature well: Role of attapulgite. *J. Pet. Sci. Eng.* **2020**, *186*, 106683.

(17) Ma, J.; An, Y.; Yu, P. Core-shell structure acrylamide copolymer grafted on nano-silica surface as an anti-calcium and anti-temperature fluid loss agent. *J. Mater. Sci.* **2019**, *54*, 5927−5941.

(18) Song, K.; Wu, Q.; Li, M.; Ren, S.; Dong, L.; Zhang, X.; Lei, T.; Kojima, Y. Water-based bentonite drilling fluids modified by novel biopolymer for minimizing fluid loss and formation damage. *Colloids Surf., A* **2016**, *507*, 58−66.

(19) Su, J.; Chu, Q.; Ren, M. Properties of high temperature resistance and salt tolerance drilling fluids incorporating acrylamide/2-acrylamido-2-methyl-1-propane sulfonic acid/N-vinylpyrrolidone/dimethyl diallyl ammonium chloride quadripolymer as fluid loss additives. *J. Polym. Eng.* **2014**, *34*, 153−159.

(20) Zhao, Z.; Pu, X.; Xiao, L.; Wang, G.; Su, J.; He, M. Synthesis and properties of high temperature resistant and salt tolerant filtrate reducer N,N-dimethylacrylamide 2-acrylamido-2-methyl-1-propyl dimethyl diallyl ammonium chloride N-vinylpyrrolidone quadripolymer. *J. Polym. Eng.* **2015**, *35*, 627−635.

(21) Bai, X.; Zhang, X.; Xu, Y.; Yong, X. Synthesis and Characterization of Sodium Carboxymethyl Starch-Graft Acrylamide/1-Vinyl-2-Pyrrolidone Copolymers via Central Composite Design and Using as Filtration Loss Agent in Drilling Muds. *Starch* **2021**, *73*, 2000151.

(22) Aflaki Jalali, M.; Dadvand Koohi, A.; Sheykhan, M. Experimental study of the removal of copper ions using hydrogels of xanthan, 2-acrylamido-2-methyl-1-propane sulfonic acid, montmorillonite: Kinetic and equilibrium study. *Carbohydr. Polym.* **2016**, *142*, 124−132.

(23) Kumar, A.; Singh, K.; Ahuja, M. Xanthan-g-poly(acrylamide): Microwave-assisted synthesis, characterization and in vitro release behavior. *Carbohydr. Polym.* **2009**, *76*, 261−267.
(24) Ghaderi, S.; Ramazani, A. S. A.; Haddadi, S. A. Applications of highly salt and highly temperature resistance terpolymer of acrylamide/styrene/maleic anhydride monomers as a rheological modifier: Rheological and corrosion protection properties studies. *J. Mol. Liq.* **2019**, *294*, 111635.
(25) Mittal, H.; Babu, R.; Alhassan, S. M. Utilization of gum xanthan based superporous hydrogels for the effective removal of methyl violet from aqueous solution. *Int. J. Biol. Macromol.* **2020**, *143*, 413−423.
(26) Pandey, S.; Do, J. Y.; Kim, J.; Kang, M. Fast and highly efficient catalytic degradation of dyes using kappa-carrageenan stabilized silver nanoparticles nanocatalyst. *Carbohydr. Polym.* **2020**, *230*, 115597.
(27) Pandey, S.; Do, J. Y.; Kim, J.; Kang, M. Fast and highly efficient removal of dye from aqueous solution using natural locust bean gum based hydrogels as adsorbent. *Int. J. Biol. Macromol.* **2020**, *143*, 60−75.
(28) Airong, W.; Haixin, S.; Zhangfa, T.; Zimin, W.; Weijian, W. Preparation and properties of KH570-AM-starch graft copolymer as filtrate reducing agents. *Chem. Ind. Eng. Prog.* **2018**, *37*, 4022−4028.
(29) Nie, J. *Study on High Temperature Resistant Xanthan Gum Based Thickener for Oil Well Cement Slurry*; Tianjin University, 2013.
(30) Ding, W.; Ha, Y.; Li, Y.; Bao, Y.; Li, Y. Synthesis and Structural Properties of Xanthan Gum-g-N-vinylpyrrolidone Graft Copolymer Prepared by Radiation. *J. Nucl. Agric. Sci.* **2016**, *30*, 695−703.
(31) Quan, H.; Hu, Y.; Huang, Z.; Wenmeng, D. Preparation and property evaluation of a hydrophobically modified xanthan gum XG-C16. *J. Dispersion Sci. Technol.* **2020**, *41*, 656−666.
(32) An, Y.; Jiang, G.; Qi, Y.; Ge, Q.; Zhang, L. Nano-fluid loss agent based on an acrylamide based copolymer "grafted" on a modified silica surface. *RSC Adv.* **2016**, *6*, 17246−17255.
(33) Zhong, H.; Qiu, Z.; Huang, W.; Cao, J. Shale inhibitive properties of polyether diamine in water-based drilling fluid. *J. Pet. Sci. Eng.* **2011**, *78*, 510−515.
(34) Faria, S.; De Oliveira Petkowicz, C. L.; de Morais, S. A. L.; Terrones, M. G. H.; De Resende, M. M.; de França, F. P.; Cardoso, V. L. Characterization of xanthan gum produced from sugar cane broth. *Carbohydr. Polym.* **2011**, *86*, 469−476.
(35) Hamcerencu, M.; Desbrieres, J.; Popa, M.; Khoukh, A.; Riess, G. New unsaturated derivatives of Xanthan gum: Synthesis and characterization. *Polym* **2007**, *48*, 1921−1929.
(36) Wang, X.; Xin, H.; Zhu, Y.; Chen, W.; Tang, E.; Zhang, J.; Tan, Y. Synthesis and characterization of modified xanthan gum using poly(maleic anhydride/1-octadecene). *Colloid Polym. Sci.* **2016**, *294*, 1333−1341.
(37) Zhongjin, L.; Yiyang, L.; Xifeng, W.; Qianfei, Z. Preparation and characterization of xanthan gum-g-P(AA-co-AMPS)/bentonite composition superabsorbent resin. *Spec. Petrochem.* **2012**, *29*, 70−73.
(38) Huang, Y.; Zhang, D.; Zheng, W. Synthetic copolymer (AM/AMPS/DMDAAC/SSS) as rheology modifier and fluid loss additive at HTHP for water-based drilling fluids. *J. Appl. Polym. Sci.* **2019**, *136*, 47813.
(39) Makhado, E.; Pandey, S.; Nomngongo, P. N.; Ramontja, J. Fast microwave-assisted green synthesis of xanthan gum grafted acrylic acid for enhanced methylene blue dye removal from aqueous solution. *Carbohydr. Polym.* **2017**, *176*, 315−326.
(40) Srivastava, A.; Behari, K. Modification of Natural Polymer Via Free Radical Graft Copolymerization of 2-Acrylamido-2-Methyl-1-Propane Sulfonic Acid in Aqueous Media and Study of Swelling and Metal Ion Sorption Behavior. *J. Appl. Polym. Sci.* **2009**, *114*, 1426−1434.
(41) Hassani, A. H.; Ghazanfari, M. H. Improvement of non-aqueous colloidal gas aphron-based drilling fluids properties: Role of hydrophobic nanoparticles. *J. Nat. Gas Sci. Eng.* **2017**, *42*, 1−12.
(42) Zhu, W.; Zheng, X.; Shi, J.; Wang, Y. A high-temperature resistant colloid gas aphron drilling fluid system prepared by using a novel graft copolymer xanthan gum-AA/AM/AMPS. *J. Pet. Sci. Eng.* **2021**, *205*, 108821.
(43) Darley, H. C. H. G.; George, R. *Composition and Properties of Drilling and Completion Fluids*; Gulf Publishing Company, 1988.
(44) Zoveidavianpoor, M.; Samsuri, A. The use of nano-sized Tapioca starch as a natural water-soluble polymer for filtration control in water-based drilling muds. *J. Nat. Gas Sci. Eng.* **2016**, *34*, 832−840.
(45) Ma, J.; Xia, B.; Yu, P.; An, Y. Comparison of an Emulsion- and Solution-Prepared Acrylamide/AMPS Copolymer for a Fluid Loss Agent in Drilling Fluid. *ACS Omega* **2020**, *5*, 12892−12904.
(46) Xiaofei, C.; Fan, L.; Bitao, S.; Huzi, W.; Boyang, L. Preparation and Performance of PAMAP Filter Loss Reducer With High Temperature and Salt resistant. *Spec. Petrochem.* **2020**, *37*, 36−40.
(47) Lu, J.; Su, J.; Wang, L.; Yu, H.; Huang, J. Effect of Treating Chemical on Colloid Stability of Drilling Polysulfonate Fluid System. *Oilfield Chem.* **2017**, *34*, 571−575.
(48) Yao, R.; Jiang, G.; Li, W.; Deng, T.; Zhang, H. Effect of water-based drilling fluid components on filter cake structure. *Powder Technol* **2014**, *262*, 51−61.
(49) Jia, H.; Huang, P.; Wang, Q.; Han, Y.; Wang, S.; Zhang, F.; Pan, W.; Lv, K. Investigation of inhibition mechanism of three deep eutectic solvents as potential shale inhibitors in water-based drilling fluids. *Fuel* **2019**, *244*, 403−411.
(50) Yang, L.; Yang, X.; Jiang, G.; Shi, Y.; Wang, T. A High Temperature Calcium Resistant Filter Loss Reducer Containing Ionic Liquid Segments. *Drill. Fluid Completion Fluid* **2018**, *35*, 8−14.
(51) Sun, J.; Xianbin, H.; Kaihe, L.; Zihua, S.; Xu, M.; Jintang, W.; Wei, L. Methods, technical progress and research advance of improving high-temperature stability of water based drilling fluids. *J. China Univ. Pet.* **2019**, *43*, 73−81.

https://doi.org/10.1021/acsomega.1c02617
ACS Omega 2021, 6, 23788−23801